Pergamon

Int. J. Heat Mass Transfer. Vol. 38, No. 9, pp. 1619–1625, 1995

0017-9310/95 $9.50+0.00

0017-9310(94)00269-X

Laminar flow heat transfer in pipes including two-dimensional wall and fluid axial conduction

ŞEFİK BİLİR

Department of Mechanical Engineering, Selçuk University, 42040 Konya, Turkey

(*Received* 22 *September* 1992 *and in final form* 15 *August* 1994)

Abstract—An analysis is made for a conjugate heat transfer problem with thermally developing laminar pipe flow, involving two-dimensional wall and axial fluid conduction. The problem is solved numerically by a finite-difference method for a thick walled, two-regional pipe which has constant outside surface temperatures interfaced by a step change. An exact profile is used to discretize the differential equation in the fluid region, and the method exhibited a simple and fast tool to solve this highly complicated problem. The effects of the three defining parameters, the Péclet number, thickness ratio and wall-to-fluid conductivity ratio, are investigated, and it is observed that the most significant of these parameters is the Péclet number, in its effective range ($Pe \leqslant 20$).

INTRODUCTION

Conjugate heat transfer problems in laminar duct flow had received little consideration up to the 1980s, as pointed out in the monograph of Shah and London [1]. In recent years, however, there have been several attempts to solve these types of problems with different sets of boundary conditions.

Mori *et al.* [2, 3] investigated the wall conduction effects between parallel plates and in circular pipes both for constant surface temperature and uniform heat flux boundary conditions. Davis and Gill [4] considered Couette flow between parallel plates to analyse the effect of axial wall conduction. Sparrow and Faghri [5] made an analysis for vertical pipes with internal forced and external natural convection. The same boundary condition for the external surface was also used by Sunden [6] for horizontal multilayer pipes, and by Wijeysundera [7] for a pipe which has a finite heated section. Thick walled pipes exhibiting two-dimensional conduction were investigated by Barozzi and Pagliarini [8] and by Campo and Shuler [9] using numerical methods.

In problems which are referred to as conjugate, the dependence of the thermal properties of the fluid on the properties of the wall is large in the thermal entrance region for a duct flow. However, when the Péclet number of the flow is low, there is also a considerable amount of axial conduction in the fluid for thermally developing flows. The coupled effect of wall and fluid axial conduction was investigated by Faghri and Sparrow [10] and Zariffeh *et al.* [11] using a finite-difference method and by Campo and Rangel [12] analytically. All these investigators considered one-dimensional conduction in the wall.

In this paper the combined effect of two-dimensional wall conduction and fluid axial conduction is analysed for low Péclet number laminar flow heat transfer. A two-regional thick-walled pipe is considered, as shown in Fig. 1. The pipe extends infinitely both in the positive and the negative directions. The external temperature of the wall in the upstream and in the downstream portions of the pipe are assumed to be constant and have different values with a jump at the beginning of the heating section. The far upstream temperature of the fluid is uniform over the section and equal to the outside wall temperature of that portion. The flow is hydrodynamically developed and physical properties of the fluid are constant. Viscous dissipation is neglected.

PROBLEM FORMULATION

Under the assumed conditions, the governing equations and the boundary conditions in non-dimensional form are as follows.

In the wall region,

$$\frac{1}{r'}\frac{\partial}{\partial r'}\left(r'\frac{\partial T'}{\partial r'}\right)+\frac{1}{Pe^2}\frac{\partial^2 T'}{\partial x'^2}=0 \qquad (1a)$$

$$\text{at} \quad x'=-\infty \quad T'=0 \qquad (1b)$$

$$\text{at} \quad x'=+\infty \quad T'=1 \qquad (1c)$$

$$\text{at} \quad r'=1+t' \quad \text{for} \quad x'<0 \quad T'=0 \qquad (1d)$$

$$\text{at} \quad r'=1+t' \quad \text{for} \quad x'\geqslant 0 \quad T'=1 \qquad (1e)$$

$$\text{at} \quad r'=1 \quad T'_{\mathrm{s}}=T'_{\mathrm{f}} \quad \text{and} \quad \left(\frac{\partial T'}{\partial r'}\right)_{\mathrm{s}}=\frac{1}{k_{\mathrm{sf}}}\left(\frac{\partial T'}{\partial r'}\right)_{\mathrm{f}}. \qquad (1f,g)$$

In the fluid region,

$$(1-r'^2)\frac{\partial T'}{\partial x'}=\frac{1}{r'}\frac{\partial}{\partial r'}\left(r'\frac{\partial T'}{\partial r'}\right)+\frac{1}{Pe^2}\frac{\partial^2 T'}{\partial x'^2} \qquad (2a)$$

NOMENCLATURE

c_p	specific heat at constant pressure
k	thermal conductivity
L	length, defined by equation (7)
Nu	Nusselt number
Pe	Péclet number
q	heat flux
r	radial coordinate
T	temperature
t	thickness of the pipe wall
u	velocity in the axial direction
x	axial coordinate.

Greek symbols

δr	radial position difference
δx	axial position difference
Δr	radial step size
Δx	axial step size
ρ	density.

Subscripts

b	bulk
i, j	at nodal point i, j
f	fluid
m	mean
r	radial
s	solid
sf	ratio of solid to fluid
w	at solid–fluid interface
x	axial.

Superscript

′	dimensionless quantity.

$$\text{at} \quad x' = -\infty \quad T' = 0 \tag{2b}$$

$$\text{at} \quad x' = +\infty \quad T' = 1 \tag{2c}$$

$$\text{at} \quad r' = 0 \quad \frac{\partial T'}{\partial r'} = 0 \tag{2d}$$

$$\text{at} \quad r' = 1 \quad T'_f = T'_s \quad \text{and} \quad \left(\frac{\partial T'}{\partial r'}\right)_f = k_{sf}\left(\frac{\partial T'}{\partial r'}\right)_s. \tag{2e, f}$$

The dimensionless variables are defined as

$$T' = \frac{T - T_0}{T_1 - T_0} \quad x' = \frac{x}{r_w Pe} \quad r' = \frac{r}{r_w} \quad t' = \frac{t}{r_w} \quad k_{sf} = \frac{k_s}{k_f}$$

and

$$Pe = \frac{2u_m r_w \rho c_p}{k_f}.$$

The fluid bulk temperatures and local Nusselt numbers may be computed from

$$T'_b = 4\int_0^1 r'(1 - r'^2)T' \, dr' \tag{3}$$

$$q_w = \left(\frac{\partial T'}{\partial r'}\right)_{r'=1} \tag{4}$$

and

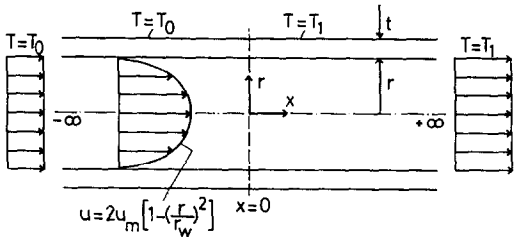

Fig. 1. Schematic diagram of the problem and coordinate system.

$$Nu = \frac{-2q_w}{T'_w - T'_b}. \tag{5}$$

SOLUTION METHODOLOGY

Solutions of the problem defined by the system of equations (1) and (2) are obtained numerically by using a finite-difference method. Equation (1) in the solid region is discretized by the so-called central-difference profiles since there are only conductive terms in it. Equation (2), however, is discretized in a different manner, since it contains both conductive and convective terms in the axial direction.

For convergence in convection problems, central-difference profiles are safely used when the Péclet number of the flow is very small ($Pe < 2$) or by using very fine grids [13]. The upwind scheme, on the other hand, gives satisfactory results only for large Péclet number flows ($Pe > 50$) for it assumes zero conduction. However, the effect of fluid axial conduction is important, especially for flows with $Pe < 50$. Therefore, a better profile should be used to characterize the temperature change in the flow direction in the fluid region. Such a profile was developed in a similar problem and the details of the derivation of the pertinent difference equations are given in ref. [14]. An outline of the procedure is as follows.

If the terms in x-direction of equation (2) is grouped and equated to zero, the equation for the one-dimensional version of the convection–conduction problem in the fluid region is obtained:

$$(1 - r'^2)\frac{dT'}{dx'} - \frac{1}{Pe^2}\frac{d^2T'}{dx'^2} = 0. \tag{6}$$

The solution of the above equation in a domain like $0 \leqslant x' \leqslant L'$ and by assuming that $T'(0) = T'_0$ and $T'(L') = T'_{L'}$ gives

$$\frac{T'-T'_0}{T'_{L'}-T'_0}=\frac{\exp[Pe^2(1-r'^2)x']-1}{\exp[Pe^2(1-r'^2)L']-1}. \quad (7)$$

If this profile is applied to adjacent grid points in the flow direction and combined with the central-difference profiles in the radial direction, the following discretization equation is obtained for a nodal point (i, j) in the fluid region:

$$a_{i,j}T'_{i,j}=b_{i,j}T'_{i+1,j}+c_{i,j}T'_{i-1,j}+d_{i,j}T'_{i,j+1}+e_{i,j}T'_{i,j-1} \quad (8a)$$

where

$$b_{i,j}=\frac{(r'_{i,j}-r'^3_{i,j})(\Delta r')_{i,j}}{\exp[Pe^2(1-r'^2_{i,j})(\delta x')_{i+1,j}]-1} \quad (8b)$$

$$c_{i,j}=\frac{(r'_{i,j}-r'^3_{i,j})\exp[Pe^2(1-r'^2_{i,j})(\delta x')_{i-1,j}](\Delta r')_{i,j}}{\exp[Pe^2(1-r'^2_{i,j})(\delta x')_{i-1,j}]-1} \quad (8c)$$

$$d_{i,j}=\frac{r'_{i,j+1}}{(\delta r')_{i,j+1}}(\Delta x')_{i,j} \quad (8d)$$

$$e_{i,j}=\frac{r'_{i,j-1}}{(\delta r')_{i,j-1}}(\Delta x')_{i,j} \quad (8e)$$

$$a_{i,j}=b_{i,j}+c_{i,j}+d_{i,j}+e_{i,j}. \quad (8f)$$

This method of discretization may be treated as an application of the general method defined as an exact or exponential scheme by Patankar [13].

The temperature distribution was computed by the Gauss–Seidel iteration technique. Radially, the computational region is limited in one direction by the outside wall surface and by the axis in the other. The axial distances, on the other hand, for both the upstream and the downstream directions are estimated by pre-runs with coarse grids, in order to find the locations where the boundary conditions at $x=-\infty$ and $x=+\infty$ are satisfied.

The grid points are located both in the wall and in the fluid regions. To enhance the accuracy, the grids are contracted in r-direction near the solid–fluid interface in both solid and fluid regions. The contraction of the grids are also applied in the x-direction around the beginning of the heating zone ($x=0$) in both upstream and downstream directions. Moreover the grid sizes in the axial direction were varied by linearly stretching the axial coordinate, i.e. the axial step size of a grid was taken as 1.5 times the step size of the previous grid, starting at $x=0$ and increasing in both upstream and downstream directions. The minimum step size used in the axial direction is 0.0001, while it is $t'/8$ in the radial direction. Satisfactory results were obtained by using to a total of 12 grid spacings (four in the wall and eight in the fluid region) in the r-direction. A total number of 22–28 grid points were used in the x-direction, depending on the axial length of the computational region, which depends on the parameters of the problem.

During an iteration, the information was transferred between the solid and the fluid regions via conditions (1g) and (2e). A consecutive procedure was used in the calculations. For a typical run, the temperature distribution in the solid region was found by using the temperature distribution of the previous run and by condition (1g) at the interface. Then, iteration was continued on the fluid side using the temperature distribution of the inner surface as a boundary condition (2e). Therefore, the information was carried from solid to fluid domain by the interface temperatures, and from fluid to solid by the heat fluxes.

The iterations were continued until convergence up to the fifth decimal figures was achieved. To increase the rate of convergence, the points are visited by a traverse direction from outer wall to axis and by a sweep direction from upstream to downstream. A relaxation factor of 1.5 was used throughout the calculations. The rate of convergence was quite rapid, and, depending on the parameters, the solutions were obtained within 60 to 230 iterations. A micro-PC was used for the calculations.

Accuracy tests were performed by increasing the number of grid points up to 16 times; by increasing the convergence limit up to the seventh decimal figure; by changing the locations of the grid points, the initially guessed temperature field and by reversing the traverse and sweep directions during the calculations. The maximum difference in the calculated values for any of these cases was not more than 2%.

RESULTS AND DISCUSSION

The results of the problem depend on three parameters, Pe, t' and k_{sf}. Calculations were then made for several combinations of these parameters. For the Péclet number the values of 1, 5 and 20 are used, since axial fluid conduction is not negligible for flows of this range. Three different values are also used for the thickness ratio, 0.02, 0.1 and 0.3, appropriate for problems of engineering interest.

Low Péclet number flow and therefore axial fluid conduction is generally assumed to be a characteristic of low Prandtl number fluids such as liquid metals. These fluids, however, possess high thermal conductivity, and the expected wall-to-fluid conductivity ratio should not have very large values. On the other hand, calculations using very large values of k_{sf} would give a chance to make a comparison, since very large k_{sf} corresponds to the situation of very small or no wall resistance. Calculations were then made for k_{sf} values of 1, 10, 100 and 10^4. The results of the calculations, however, indicate that the computed values are invariably close for the cases of $k_{sf}=100$ and $k_{sf}=10^4$ for any combinations of the other two variables. To see further how solutions are changed with k_{sf}, some runs were performed and it was seen that, when k_{sf} exceeds 100, any change of this parameter has almost no effect.

Similarly, to obtain the limiting values of t' and Pe,

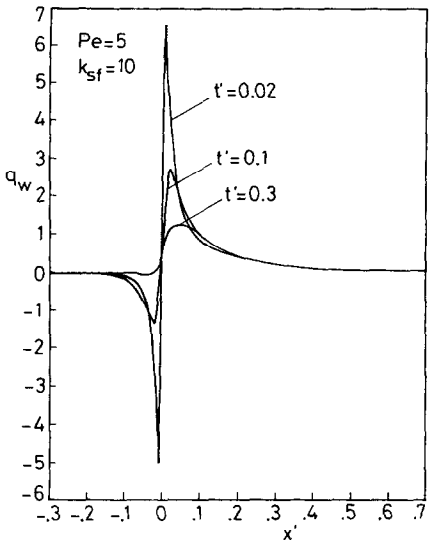

Fig. 2. Effect of thickness ratio on interfacial heat flux.

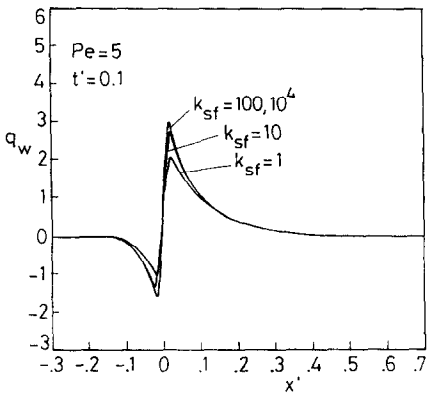

Fig. 3. Effect of conductivity ratio on interfacial heat flux.

beyond which the calculated values are not affected, runs were performed for some small values of wall thickness up to $t' = 10^{-4}$ and for some large values of the Péclet number up to $Pe = 500$. When wall thickness is small, wall conduction effects decrease and the results approach the case of no wall conduction. On the other hand, when the Péclet number increases, both fluid axial conduction and wall conduction effects are negligible, and the results get closer to the case of no wall and fluid axial conduction. The results indicate that with the boundary conditions of the present conjugated problem, the change in the computed values may be assumed negligible when $k_{sf} > 100$, $Pe > 20$ and $t' < 0.02$.

The local Nusselt number, as traditionally considered in the presentation of the convection heat transfer results, is not a convenient tool for the conjugate problems, since it contains three unknowns in its definition [10]. The local interfacial heat flux gives more meaningful information, and therefore the results are presented by and the discussions are mainly based on local interfacial heat flux values. However, some results are also given in terms of fluid bulk temperatures, local Nusselt numbers and inner wall temperatures, in order to better understand the nature of the conjugated problem. On the other hand, the only comparable results in the available literature are given in ref. [15] in terms of bulk temperatures and local Nusselt numbers. Therefore the results of the present work are compared by means of these parameters.

Figures 2–4 present axial distribution of interfacial heat flux values. A parametric representation is given in these figures to analyse the effects of each defining parameter.

In Fig. 2 interfacial heat flux values are given for $Pe = 5$, $k_{sf} = 10$ and for three different values of t'. Inspection of this figure will also show the general trend of all q_w curves as well as the effect of the thickness ratio on conjugated heat transfer. As can be seen, there is a substantial amount of heat transfer occurring in the upstream region due to the penetration of heat opposite to the direction of flow, resulting from axial wall and fluid conduction. In the vicinity of the beginning of the heating section of the pipe ($x = 0$), the upstream heat flux values are positive, i.e. from wall to the fluid: however, further upstream they become negative. In the wall region, heat penetrated through the upstream side is lost from the outside surface and fluid temperatures adjacent to the inner wall of the pipe, where convection vanishes, may be higher than the inner wall temperatures, leading to reverse heat transfer. The amount of reverse heat flux in the upstream section decreases with increasing upstream distance and ceases to zero. Since thick walls exhibit more axial conduction, both the extent and the magnitude of reverse heat transfer is smaller.

In the downstream side of the pipe the curves rise to a maximum value and then decrease. The reason for such a peak may be explained by high temperature gradients at the beginning of the heating section. The thermal resistance of the pipe wall is smaller for thin walls and heat supplied from the outer surface is easily transferred to the inner surface. Therefore the peak heat flux values are higher for small wall thickness.

At the beginning of the heating section, wall conduction is dominant over convection and the heat

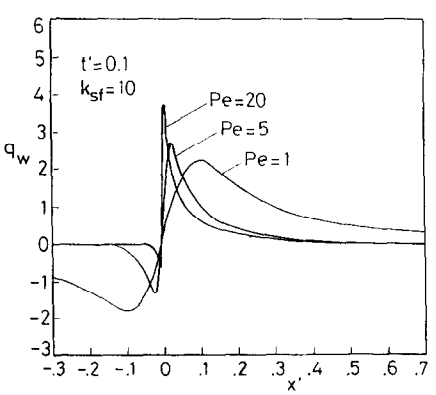

Fig. 4. Effect of Péclet number on interfacial heat flux.

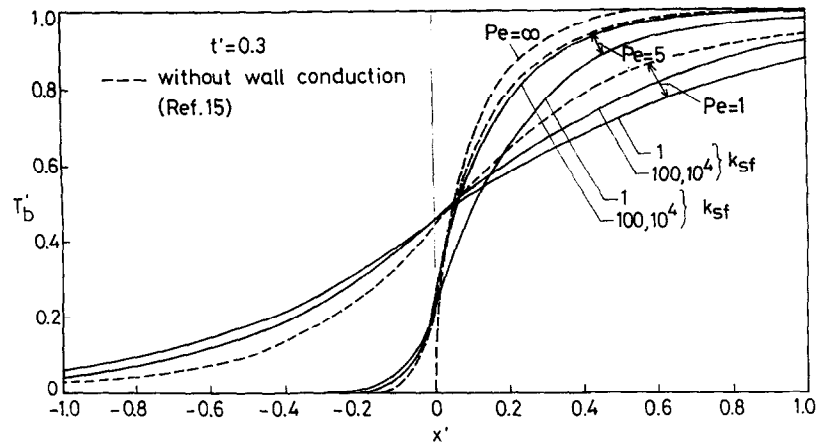

Fig. 5. Axial distribution of the fluid bulk temperature ($t' = 0.3$).

flux values are high. After a certain axial distance is reached, convection is more pronounced and heat flux values decrease. The above described trend is stronger for thin walls, and therefore the peak value of heat flux occurs at smaller axial distances. For this reason, the curves cross at some axial distance downstream of the pipe. The extent of the downstream heating or the development length is slightly increased with increasing wall thickness due to more axial wall conduction.

In Fig. 3 the effect of wall-to-fluid thermal conductivity ratio on interfacial heat flux is shown. The amount of reverse heat transfer in the upstream region is greater with large k_{sf}. Since large k_{sf} means small thermal resistance in the wall, interfacial temperatures and therefore heat flux values are large in the heated section. Both the extent of upstream heat transfer and the development length in the downstream region are almost the same for all k_{sf} values.

For large values of conductivity ratio, heat supplied from the outer wall surface is easily transferred in radial direction to the inner wall surface and therefore both the extent and the magnitude of the backward axial conduction decrease. This causes lower interfacial temperatures in the upstream side, resulting in higher values of reverse heat transfer in the upstream side for large k_{sf}.

In order to investigate the effect of Péclet number, Fig. 4 is drawn for axial distribution of interfacial heat flux for different Péclet numbers. In the upstream side, the extent and the magnitude of reverse heat flux are increased with decreasing Péclet number. This is due to the large amounts of axial fluid conduction and penetration of heat backward through the upstream side for small Péclet number flows. The extent of post-heating in the downstream section is also increased with decreasing Péclet number, since the convective effect is low and therefore the development length is increased. The degree of peak is smaller and the drop-off is more gradual in heat flux values with small Péclet numbers.

Fluid bulk temperatures are given in Figs. 5 and 6. In Fig. 5 the curves are given for the same thickness ratio but for different Pe and k_{sf} values. Figure 6, however, is drawn for the same conductivity ratio but with different t' and Pe values. The two figures compare the effect of each parameter on bulk temperatures. As wall axial conduction increases (greater t', smaller k_{sf}), and as fluid axial conduction increases

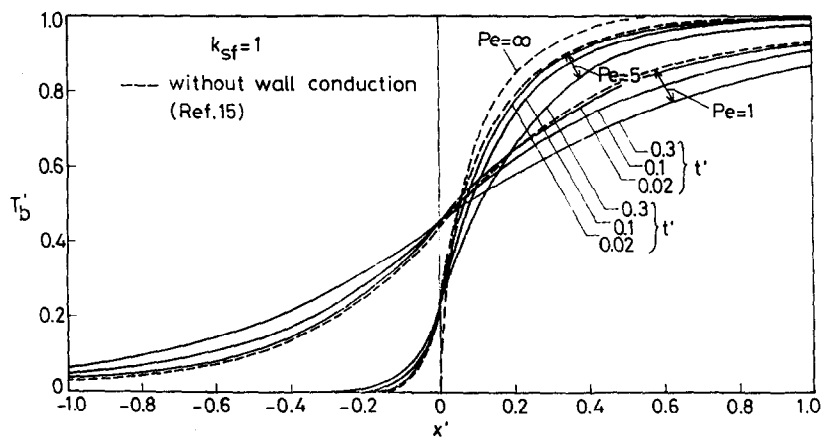

Fig. 6. Axial distribution of the fluid bulk temperature ($k_{sf} = 1$).

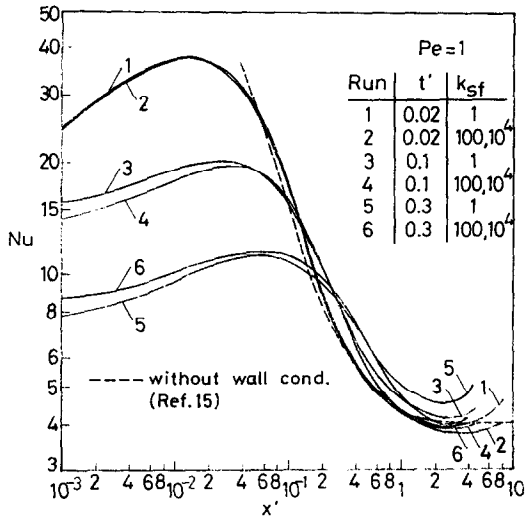

Fig. 7. Axial distribution of the local Nusselt number ($Pe = 1$).

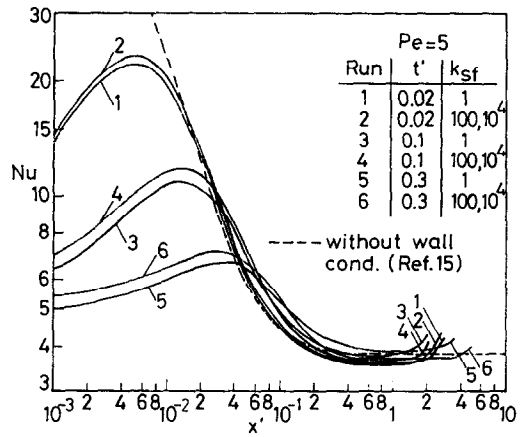

Fig. 8. Axial distribution of the local Nusselt number ($Pe = 5$).

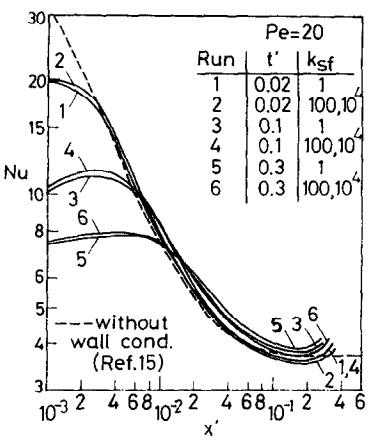

Fig. 9. Axial distribution of the local Nusselt number ($Pe = 20$).

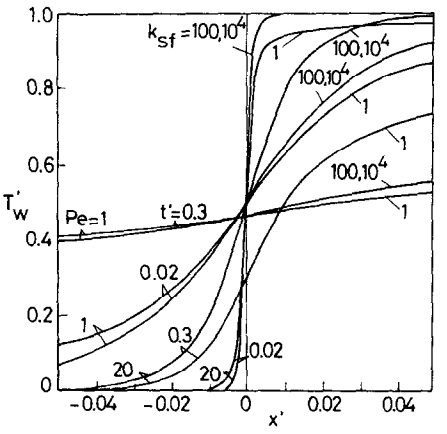

Fig. 10. Axial distribution of the inner wall temperature.

(smaller Pe), the diffusion of heat into the upstream side increases the bulk temperatures in this region and decreases those in the downstream region. The curves get closer to the case of no wall conduction with decreasing t' and increasing k_{sf}, and to the case of no wall and fluid axial conduction ($Pe = \infty$) for large Péclet numbers.

Local Nusselt numbers for the downstream region are drawn in Figs. 7–9. Each of these figures are parameterized with different t' and k_{sf} values for the same Péclet number. In the vicinity of the heated section, the local Nusselt numbers are smaller than those for the case of no wall conduction and the curves rise to a maximum and then decrease. The reason for such a peak is due to the similar behaviour of q_w curves, since q_w is a defining parameter of the Nusselt number [equation (5)]. The degree of peak is smaller and is shifted downstream with increasing wall thickness and with decreasing k_{sf} as in q_w curves. Reverse heat transfer from fluid to the wall in the upstream side and low heat flux values at the beginning of the heated section extend the heat transfer further downstream. This causes the interfacial heat flux and therefore the local Nusselt numbers to become higher than those of the no wall conduction case after a certain axial distance. This trend is more influenced in thick walled pipes and with lower k_{sf} values, and therefore the Nusselt curves cross at some axial distance.

Another interesting feature of the Nusselt curves is that, far downstream, instead of reaching an asymptotic fully developed value, they attain a minimum and then begin to rise. Such a rise in Nusselt values is indicated in some conjugated problems, as is also reported in refs. [5, 11]. The values of the minima change with parameters and, for some cases, may be less than the asymptotic value of the case of no wall conduction.

Finally, inspection of Figs. 7–9 shows that the effect of wall conduction on local Nusselt numbers is more pronounced with low Péclet number flows and may be assumed negligible for flows with $Pe > 20$, except in the immediate vicinity of $x = 0$.

Inner wall temperature distributions, again for some representative groups of parameters, are given in Fig. 10. Inspection of the curves reveals that an increase either in wall axial conduction (large t', small

k_{sf}) or fluid axial conduction (small Pe) increases internal wall temperatures in the upstream side and decreases those in the downstream side. Since the dimensionless outer wall temperature is 0 in the upstream side and 1 in the downstream side of the pipe, the difference between the inner and the outer wall temperatures is high around $x = 0$. Another point which can be deduced from this figure is that the effect of k_{sf} on internal wall temperature is increased with decreasing axial fluid conduction.

CONCLUDING REMARKS

A simple and fast numerical procedure is used to solve a conjugated heat transfer problem for laminar pipe flows including two-dimensional wall and fluid axial conduction. Heat transfer parameters depend on three dimensionless groups, Pe, t' and k_{sf}. The main conclusions of the investigation are as follows:

(1) The effect of wall conduction on heat transfer increases with increasing t' and with decreasing Pe and k_{sf}.

(2) The change in the computed values is not significant under a change of each of the parameters when $Pe > 20$, $k_{sf} > 100$ and $t' < 0.02$.

(3) With the boundary conditions of the present conjugated problem, the Péclet number in its effective range ($Pe < 20$), or in other words the axial fluid conduction has the dominant influence on heat transfer. This indicates that the results are mainly depended on flow conditions rather than on the wall characteristics.

(4) The effect of k_{sf} is more pronounced when the thickness ratio and Péclet number increase. The effects of Pe and t', however, are approximately unchanged, irrespective of the orders of the other parameters in their significant range.

REFERENCES

1. R. K. Shah and A. L. London, *Laminar Flow Forced Convection in Ducts*. Academic Press, New York (1978).
2. S. Mori, T. Shinke, M. Sakakibara and A. Tanimoto, Steady heat transfer to laminar flow between parallel plates with conduction in wall, *Heat Transfer Jap. Res.* **5,** 17–25 (1976).
3. S. Mori, M. Sakakibara and A. Tanimoto, Steady heat transfer to laminar flow in a circular tube with conduction in tube wall, *Heat Transfer Jap. Res.* **3,** 37–46 (1974).
4. E. J. Davis and N. W. Gill, The effects of axial conduction in the wall on heat transfer with laminar flow, *Int. J. Heat Mass Transfer* **13,** 459–470 (1970).
5. E. M. Sparrow and M. Faghri, Fluid-to-fluid conjugate heat transfer for a vertical pipe—internal forced convection and external natural convection, *Trans. ASME J. Heat Transfer* **102,** 402–407 (1980).
6. B. Sunden, Conjugated heat transfer from circular cylinders in low Reynolds number flow, *Int. J. Heat Mass Transfer* **23,** 1359–1367 (1980).
7. N. J. Wijeysundera, Laminar forced convection in circular and flat ducts with wall axial conduction and external convection, *Int. J. Heat Mass Transfer* **29,** 797–807 (1986).
8. G. S. Barozzi and G. Pagliarini, A method to solve conjugate heat transfer problems: the case of fully developed laminar flow in a pipe, *Trans. ASME J. Heat Transfer* **107,** 77–83 (1985).
9. A. Campo and C. Shuler, Heat transfer in laminar flow through circular tubes accounting for two-dimensional wall conduction, *Int. J. Heat Mass Transfer* **31,** 2251–2259 (1988).
10. M. Faghri and E. M. Sparrow, Simultaneous wall and fluid axial conduction in laminar pipe-flow heat transfer, *Trans. ASME J. Heat Transfer* **102,** 58–63 (1980).
11. E. K. Zariffeh, H. M. Soliman and A. C. Trupp, The combined effects of wall and fluid axial conduction on laminar heat transfer in circular tubes, *Heat Transfer* **4,** 131–135 (1982).
12. A. Campo and R. Rangel, Lumped system analyses for the simultaneous wall and fluid axial conduction in laminar pipe flow heat transfer, *PhysicoChem. Hydrodyn.* **4,** 163–173 (1983).
13. S. V. Patankar, *Numerical Heat Transfer and Fluid Flow*. Hemisphere, Washington, DC (1980).
14. Ş. Bilir, Numerical solution of Graetz problem with axial conduction, *Numer. Heat Transfer Pt A* **21,** 493–500 (1992).
15. D. K. Hennecke, Heat transfer by Hagen Poiseuille flow in the thermal development region with axial conduction, *Wärme- und Stoffübertragung* **1,** 177–184 (1968).